CRACKING OF MASONRY ARCHES WITH GREAT DEFORMATIONS:
A NEW EQUILIBRIUM APPROACH

José Ignacio Hernando García, Fernando Magdalena Layos and Antonio Aznar López

msp

CRACKING OF MASONRY ARCHES WITH GREAT DEFORMATIONS: A NEW EQUILIBRIUM APPROACH

JOSÉ IGNACIO HERNANDO GARCÍA,
FERNANDO MAGDALENA LAYOS AND ANTONIO AZNAR LÓPEZ

Masonry arches crack inexorably after decentering. This phenomenon is well known to any master builder. For small deformations these cracks do not affect the safety of the arch. Indeed, the arch with time may show different patterns of cracking, which lead to different sets of internal forces. Within the frame of modern limit analysis, developed for masonry structures, mainly by Professor Heyman since the 1960s, we know that cracking is irrelevant to safety: indeed, it is the capacity of forming cracks which gives "plasticity" to masonry. Small deformations do not distort the overall form of the arch. A direct corollary of the safe theorem states that if it is possible to draw a line of thrust within the arch, the arch will not collapse, and it is safe. This is independent of the "actual" state of the arch, manifested by a certain pattern of cracks. This pattern will change with very small (unpredictable) variations in the boundary conditions; a tiny spreading of the abutments will produce a complete change.

However, when the deformations are large, the geometry of the arch is severely distorted and we cannot study the stability with the original geometry: it is necessary to proceed step by step, considering the deformed geometry. This phenomenon has been rarely studied. However, even these studies consider, as a simplification, that the crack patterns do not vary and the movement is studied under this assumption. That this is not the case can be seen with tests with small models of arches: the position of cracks can be altered, and this may influence the validity of the study. The present contribution proposes a method of analysis which permits us to study the history of cracking until collapse. This has not only theoretical interest; it may be used in the analysis of some critical cases which occur in practice.

1. Maximum and minimum thrust of a masonry arch: linear analysis

This work is based on three hypotheses (see [Heyman 1966; 1995; 2007]) that are assumed as valid. The discussion, as well as the validation, of them is out of the scope of the present article. These assumptions are

(1) the elements can be considered as solid rigid voussoirs because the stresses of the elements are low, despite the contact between the elements being located in a single point,

(2) sliding failure cannot occur, and

(3) masonry has no tensile strength.

The second assumption is based on the idea that arches are formed by a line sequence of voussoirs. Recent studies of systems that have a geometry with more complex topology are considered in [Fortunato et al.

2018; Portioli and Cascini 2017] and with a more theoretical approach in [Fortunato et al. 2016]. The last study focuses on a single arch, while the present work has no such limitation.

The stress in the joints of the arch (contact between voussoirs) has been described as proposed by Livesley [1978]: a shear force and two axial forces are considered at each joint.

Already Méry [1840] showed the relationship between thrust lines (equilibrium solutions) and patterns of cracking, crucially identifying the typical cracks giving the maximum and minimum thrust.

With all these premises, the calculation of the minimum horizontal thrust (h) is determined by either of the two dual problems of linear programming (LP):

$$\min h = \boldsymbol{c}^t \cdot \boldsymbol{s} \qquad \text{such that } [\boldsymbol{H}_N \ \boldsymbol{H}_V] \cdot \begin{bmatrix} \boldsymbol{s}_N \\ \boldsymbol{s}_V \end{bmatrix} = \boldsymbol{f}, \ \boldsymbol{s}_N \leq 0, \ (\boldsymbol{s}_V);$$

$$\max W_{\text{ext}} = \boldsymbol{f}^t \cdot \boldsymbol{u} \qquad \text{such that } (\boldsymbol{u}), \ \boldsymbol{H}_N^t \cdot \boldsymbol{u} \geq \boldsymbol{c}_N, \ \boldsymbol{H}_V^t \cdot \boldsymbol{u} = \boldsymbol{c}_V. \tag{1-1}$$

Here, as is usual, $\boldsymbol{f}$ represents the system forces vector, $\boldsymbol{H}$ is the equilibrium matrix, and $\boldsymbol{s}$ is the internal forces vector. In the dual kinematic formulation, $\boldsymbol{H}^t$ is the compatibility matrix and $\boldsymbol{u}$ is the movement vector. The unrestricted variables are shown in brackets for the sole purpose of underlining the symmetry between the primary static problem and the dual kinematics. Indices N and V refer to the axial and shear forces, respectively. The internal force vector $\boldsymbol{s}$ has been reordered as $\boldsymbol{s}^t = [\boldsymbol{s}_N \ \boldsymbol{s}_V]$ to clarify the constraints placed on each variable. The equilibrium matrix $\boldsymbol{H}$ and the $\boldsymbol{c}$ vector were reordered in the same way. Although it is unnecessary for the purposes of this paper, a more detailed version of the problem restrictions may be consulted in [Magdalena Layos 2013; Fishwick 1996]. An analysis of the effect of settlements in general plane masonry structures can be found in [Iannuzzo et al. 2018].

When the dummy variables are incorporated into $\boldsymbol{e} = \boldsymbol{H}^t \cdot \boldsymbol{u}$, one can write

$$\begin{bmatrix} \boldsymbol{H}_N^t \\ \boldsymbol{H}_V^t \end{bmatrix} \boldsymbol{u} = \begin{bmatrix} \boldsymbol{e}_N \\ \boldsymbol{e}_V \end{bmatrix}; \quad \boldsymbol{e}_N \geq \boldsymbol{c}_N, \quad \boldsymbol{e}_V = \boldsymbol{c}_V. \tag{1-2}$$

In order to obtain the minimum (maximum) horizontal force of the arch, the objective function of the problem is

$$h = \pm(N_i + N_j)\cos\alpha \pm V_{i,j}\sin\alpha. \tag{1-3}$$

Here the subscripts i, j refer to the vertices defining the first and last contact points of the joint of the arch, α corresponds to the angle between the plane of the joint and the horizontal line, the sign $\pm$ depends on the support — left or right — of the arch and on the criterion of the sign that has been adopted. The constraint of the kinematic equations $c_{N,i} \geq \cos\alpha$; $c_{N,j} \geq \cos\alpha$; $c_{V,ij} = \sin\alpha$ has a clear physical interpretation: the movement (horizontal) of the support of the arch has a parallel component $u_V = \cos(\alpha)$ and a perpendicular one $u_N = \sin(\alpha)$, both of them referenced to the local axis of the joint. If sliding failure cannot occur, the first component corresponds to the deformation e_V and the second one must be lower or equal to each strain e_N. Note that moreover the virtual mechanism is normalized in the kinematic formulation so that horizontal arch end movement is 1. To this end, it is supposed that the movements are sufficiently small to make this approximation possible (rigorously, the initial velocities instead of the movements should be considered, thus several references show the notation $\dot{\boldsymbol{u}}$).

For the recommended normalization of the vector $\boldsymbol{u}$ and using the virtual work principle (VWP), it is clear that the objective function of the kinematic problem $W_{\text{ext}} = \boldsymbol{f}^t \cdot \boldsymbol{u}$ coincides with minimum thrust, as the work of the internal forces will be reduced to $W_{\text{int}} = 1 \cdot h$.

It is also clear that if vector $\boldsymbol{c}$ is multiplied by a factor γ_u, the $\boldsymbol{u}_\gamma = \gamma_u \boldsymbol{u}$ vector is the solution to the new kinematic problem and the value of the target function will be $W_{\text{ext},\gamma} = \gamma_u W_{\text{ext}}$. Using the VWP again the conclusion is that

$$W_{\text{int},\gamma} = W_{ext,\gamma} \rightarrow \gamma_u(1 \cdot h) = \gamma_u W_{\text{ext}} \rightarrow h = W_{\text{ext}}, \tag{1-4}$$

i.e., that the thrust value of the arch does not vary.

Regarding the static problem scale, it is only necessary to modify the objective function $h_\gamma = \gamma_u \boldsymbol{c}^t \cdot \boldsymbol{s}$. If $\boldsymbol{s}$ is the solution of the first problem, the solution of the scaled problem corresponds to this same solution multiplied by the γ_u factor.

2. Maximum and minimum thrust of a masonry arch: nonlinear analysis

Restricting to small displacements, in the limit infinitesimal, the angle of aperture of the joints θ is small too. When two voussoirs open, a hinge is formed. Therefore we can approximate the value of $\sin\theta$ to θ and $\cos\theta$ to 1. In this way, the previous formulation reduces to the linear formulation:

$$\begin{aligned} &\text{(linear) } \max W_{\text{ext}} = \boldsymbol{f}^t \cdot \boldsymbol{u} \quad \text{such that } \boldsymbol{H}_N^t \cdot \boldsymbol{u} \geq \boldsymbol{c}_N, \ \boldsymbol{H}_V^t \cdot \boldsymbol{u} = \boldsymbol{c}_V \\ &\text{(nonlinear) } \max W_{\text{ext}} = \boldsymbol{f}^t \cdot \boldsymbol{u} \quad \text{such that } \boldsymbol{H}(\boldsymbol{u})_N^t \geq \boldsymbol{c}_N, \ \boldsymbol{H}(\boldsymbol{u})_V^t = \boldsymbol{c}_V. \end{aligned} \tag{2-1}$$

If the study is focused on noninfinitesimal movements, the change of variable $s = \sin\theta$, $c = \cos\theta$ can be applied and the function $\boldsymbol{H}(\boldsymbol{u})$ remains a linear function of c and s. However, the quadratic constraints $c^2 + s^2 = 1$ must be added as a condition to (2-1), introducing the first nonlinearity into the problem.

On the other hand, the progression of the initial small movement may produce the opening and closing of different joints of the arch. Due to this effect, the objective function experiences abrupt and instantaneous jumps. These jumps of the objective functions are due to the fact that both surfaces of each joint may continue to be in contact or not, as well as whether stress can be transmitted or not. This mechanical behavior can be characterized as a disjunctive (nonsmooth) behavior, and can be mathematically formulated through complementary constraints using bilinear functions or other equations having an equivalent complexity [Hu et al. 2012].

When both types of constrains are applied, the problem becomes NP-hard, with high computational complexity. Problems of this type may have multiple solutions, and this hinders their resolution by deterministic methods. In this case, the multiple possible solutions correspond to the different combinations of positions of the open joints that fulfill the restrictions. This occurs even if the simplification concerning the elimination of the dynamic stress is incorporated.

3. Incremental algorithm

In spite of the difficulties due to the nonlinearity of the problem, there exist different options for a possible solution (see [Gilbert and Melbourne 1994; Huerta and López 1997; Portioli and Cascini 2017]). The problem can be incrementally solved by superimposing a sequence of linear problems. At each step, when the initial problem is solved, the geometry of the arch is modified according to the solution obtained and

the process is repeated again. If γ_u, that is, the step amplitude of the displacement, is small enough then the accumulated errors remain small too. These errors, due to the linear approximation at each step, accumulate, and produce a aberration of the elements of the arch, elements that were initially considered as rigid blocks. The amplitude of such an aberration depends obviously on the value of γ_u that is used during the iteration.

These algorithms have two important disadvantages:

(1) They give only a single solution among all the possible solutions.

(2) Small variations of the initial geometry of the arch at each step can lead to important variations in the final solution.

These effects are a direct consequence of the circumstances described at the end of the Section 2, and they can be observed in some of the results shown below.

When the linear approximation is used it is assumed that $e = H^t u$, and in the cases in which the movements are not small, $e_{NL} = H^t(u)$ should be used instead. To solve the nonlinear problem is a rather difficult task, but when a specific u is obtained (for example, by solving the linear problem) calculating e_{LN} is simple: By introducing $e_r^{(t-1)} = e_{NL}^{(t-1)} - e_L^{(t-1)}$, where the subscript r is defined as a "residue", then $e_{NL}^{(t)} \approx e_L^{(t)} + e_r^{(t-1)}$. If the subscripts are omitted, one can write $e \approx e_L + e_r^{(t-1)}$; $e \approx H^t u + e_r^{(t-1)}$.

With this correction of the e vector, the linear problem at each step is solved:

$$\max W_{\text{ext}} = f^t \cdot u \quad \text{such that } e_N \geq c_N, \ e_V = c_v, \ \begin{bmatrix} e_N \\ e_V \end{bmatrix} = \begin{bmatrix} H_N^t \\ H_V^t \end{bmatrix} u + \begin{bmatrix} e_{r,N}^{(t-1)} \\ e_{r,V}^{(t-1)} \end{bmatrix}, \quad (3\text{-}1)$$

or the other option

$$\max W_{\text{ext}} = f^t \cdot u \quad \text{such that } H_N^t \cdot u \geq c_N - e_{r,N}^{(t-1)}, \ H_V^t \cdot u = c_V - e_{r,V}^{(t-1)}. \quad (3\text{-}2)$$

Note that if $e_r^{(t)} = e_r^{(t-1)}$ at the iteration t, then $e_{NL}^{(t)} = e_L^{(t)} + e_r^{(t-1)}$ and the constraint of the kinematic problem can be written as

$$\begin{bmatrix} H_N^t(u) \\ H_V^t(u) \end{bmatrix} = \begin{bmatrix} e_{NL,N} \\ e_{NL,V} \end{bmatrix}; \quad e_{NL,N} \geq c_N, \ e_{NL,V} = c_v. \quad (3\text{-}3)$$

In this way, the nonlinear equations $H(u)^t = e_{NL}$ are verified, as are the restriction constraints of the arch support.

When the iteration has been corrected, and always before calculating the next step, the equilibrium of the new geometry is checked. For that reason, a linear "kinematic" problem is solved by minimizing $f^t u$ using the new geometry with the constraint that the joints that have been opened cannot be closed. If the new geometry is equilibrated, then $f^t u$ must vanish. If it does not happen, it must be because the system becomes a mechanism, and a new equilibrated position could be found if any joint closes. In these cases, often another joint opens, and it is in this way that the positions of the hinges of the arch change.

The linear problem solved in this step is similar to (1-1): it is needed only to modify c_N. The nonzero components correspond to the deformation of the hinges. Then, a simple interpretation of the static dual problem can be extracted: The function of the static problem is a linear combination of the axial forces

applied to the vertices of the opened joints. If the equilibrium of the arch remains with hinges, the sum of these axial forces must be null. In another case, some of these axial forces must not be zero in order to enable the equilibrium. This same "incremental" process is applied to solve the new problem.

4. Results

Figure 1 shows the study of the effect of a given displacement of the left support of a semicircular arch composed of twelve voussoirs. The ratio between the interior and exterior radius is $5 : 8$. The external load applied to this model is zero, and only the weight of the arch has been considered.

Section 1 shows the classic problem of analyzing the effect of horizontal creep of an arch support and its dual problem (maximum/minimum thrust). It is obvious that to formulate the problem of the descent/ascent of one of the supports of the same arch (and its dual minimum/maximum vertical reaction), it is enough to substitute α (the angle between the plane of the joint and the horizontal line) by its complementary value in the target function definition (1-3).

In Figure 1 the abscissa represents the normalized displacements of the support of the arch, v_z/D (D being the interior diameter of the arch) and $\bar{v}_z$ has been defined as $\bar{v}_z = 10v_z/D$. In Figure 1,
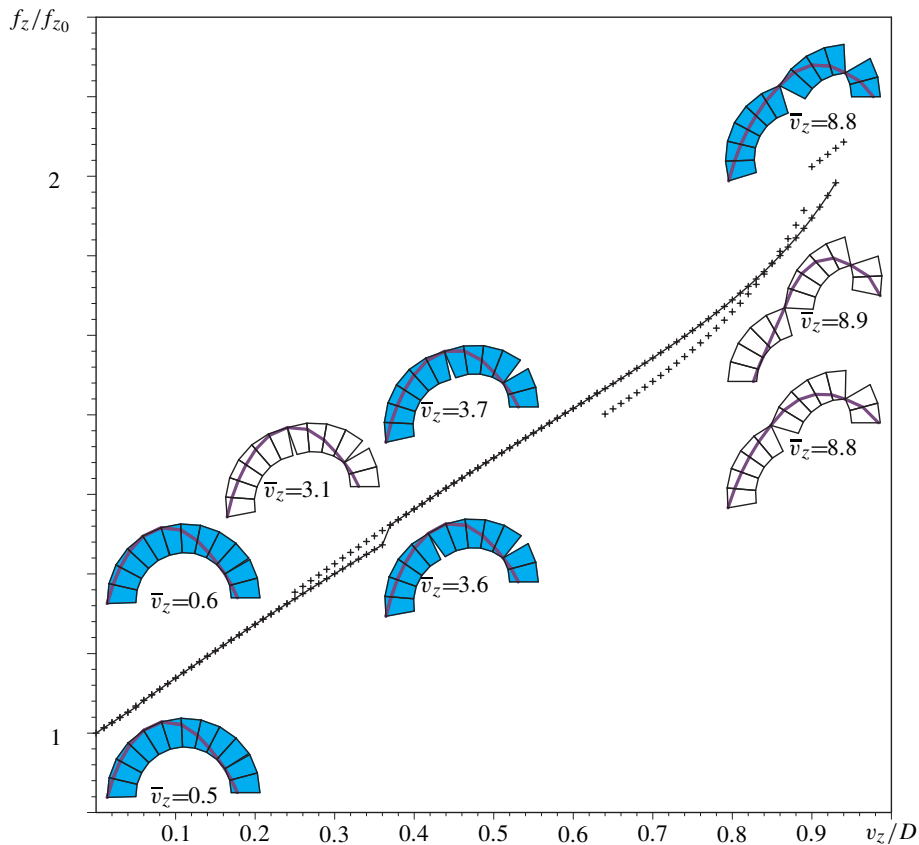
Figure 1. Variation of the vertical reaction in the left support f_z/f_{z_0} depending on the relative displacement v_z/D of the arch ($\bar{v}_z = 10v_z/D$).

the ordinate axis represents the normalized value of the vertical reaction force $f_z/f_{z,0}$, where $f_{z,0}$ is the minimum vertical reaction force calculated at the support of the arch in the initial geometry (nondeformed arch). The continuous line represented in Figure 1 has been built by applying a progressive increment in the vertical movement of the left support of the arch, and the resultant curve is similar to the curves found in [Ochsendorf 2006], in which the horizontal force of the arch is related to the horizontal displacement. In both cases, the reaction force increases when the movement advances. In this way, this movement would not stop due to the steps of Figure 1 as they have been obtained using the minimum reaction force from which the movement begins. In real masonry structures, movements like these should be due to a settlement of the foundation. In these cases, the soil would behave more or less elastic and this behavior would stop the movement of the arch unless the foundation collapses. This last consideration is difficult to justify when the horizontal movement is due to other external effects, for example, when the consequence is due to the effect of a wall, when the arch is built against a massive buttresses, etc., [Ochsendorf 2006].

The graph of Figure 1 is discontinuous, unlike the results that can be found in [Ochsendorf 2006]. This discontinuity appears at $\bar{v}_z \approx 3.7$ and $\bar{v}_z \approx 0.5$. In this last case it is more difficult to appreciate it due to the scale of the graph. Both these discontinuities correspond to steps at which the position of the hinges changes. Thus, when $\bar{v}_z = 3.6$ the sixth joint opens (between the fifth and sixth voussoirs) while when $\bar{v}_z = 3.7$ the hinge is located between the sixth and seventh voussoirs. These results are coherent with Section 2, where the nonlinearity of the problem is exposed.

In Figure 1, the geometry of the arch has been represented. In this way, the deformation at different steps of the process can be clearly observed. As can be observed, the steps corresponding to $\bar{v}_z = 0.5$, 0.6, 3.6, 3.7, 8.8 have been colored and the thrust lines have been incorporated. It can be observed that the equilibrium of the step with $\bar{v}_z = 3.6$ is tight, because the thrust line is almost tangent to the external surface of the arch near the sixth voussoir. From this step, when the position of the hinge changes, when $\bar{v}_z = 3.7$, it can be observed that the equilibrium of the arch improves.

Between the steps in which $\bar{v}_z = 0.5$ and $\bar{v}_z = 0.6$ the position of the hinge changes from the fourth-fifth voussoirs to the fifth-sixth ones. The position of the hinge when $\bar{v}_z \leq 0.5$ corresponds to the results using classic linear analysis.

From $\bar{v}_z = 3.7$ to the last step, in which the solution is located at $\bar{v}_z = 9.2$, the position of the hinges does not vary. One deformed arch in this family of results has been drawn ($\bar{v}_z = 8.8$, colored arch). If this state is compared to $\bar{v}_z = 3.7$, it can be seen that when the vertical displacement in the left support increases, the thrust lines tend to approach the right of the arch. It is easy to find the step in which collapse occurs: when the thrust line is located on the far right of the right support it is not possible to find equilibrated positions.

Additionally, the graph in Figure 1 shows the results when the direction of the movement of the right support changes from $\bar{v}_z = 3.7$ (the dashed line between $\bar{v}_z = 3.6$ and $\bar{v}_z = 2.5$). If a new analysis is performed from $\bar{v}_z = 3.7$ in order to calculate the state with lower vertical displacement of the support ($\bar{v}_z = 3.6$, $\bar{v}_z = 3.5$, etc.), a new solution is obtained that is different from the previous one (when the displacement of the support was gradually increasing). It is important to note that the position of the joints in these new solutions do not vary from the position of the state $\bar{v}_z = 3.7$. As expected in Section 2, this problem has no unique solution. One of these new solutions is represented ($\bar{v}_z = 3.1$, without color

arch). When $\bar{v}_z < 2.5$, the joint located between the sixth and seventh voussoirs returns to its original position.

Due to the similarity between both solutions (2.5, 3.6) it can be assumed that the first or second solution may be obtained indistinctly. Any small imperfection or minor perturbation could cause the change from one step to another.

In Figure 1 another second family of solutions has been shown using a dashed line. From step $\bar{v}_z = 6.4$ to $\bar{v}_z = 8.8$, solutions appear once again in which the hinges are located between the fifth and sixth voussoirs. This location continues during the entire interval (although $\bar{v}_z$ may increase or decrease the position of the hinges).

This occurs until the value decreases to $\bar{v}_z = 6.4$. It is in this step when the arch geometry is modified and the location of the hinge varies by closing the seventh joint and opening the sixth. In the following steps, the solution obtained matches the original ones (represented by the continuous line), independently of the increase or decrease in $\bar{v}_z$. From this point, it is necessary to add a new perturbation into the algorithm in order to obtain the same results again. An example of such a perturbation could be to include the prevention of the aperture in the seventh joint so that the joint can not be opened. One of the deformed arches in this family of results has been drawn, $\bar{v}_z = 8.8$ (without color). It can be observed that this step corresponds to the last one, because the thrust line reaches the right of the right support. This step is similar to the one previously described (when $\bar{v}_z = 8.8$ and the arch is colored). However, in this new point the arch has not yet collapsed. The vertical displacement can increase to $\bar{v}_z = 8.8$, further opening the right hinge and slightly closing the left one ($\bar{v}_z = 8.9$, without color arch).

These results cannot be generalized, nor can it be confirmed that the position of the hinges changes when vertical displacement increases.

Figure 2 shows the analysis of the same arch when the number of voussoirs varies. The left graph corresponds to an arch with ten voussoirs, and it can be seen that the position of the hinges does not vary until movements approach arch collapse. In this case, the location of the hinges does not depend on $\bar{v}_z$. During the last steps, when the location of the hinge varies, $\bar{v}_z = 8.1$, the left hinge closes while on contrary the right hinge opens. This effect was previously observed in analysis of the twelve voussoir arch. In this graph, different steps of the deformed arch have been represented ($\bar{v}_z = 0.1, 0.5, 8.0, 8.1$) and the main solution of Figure 1 has been included with a dashed line. The step when $\bar{v}_z = 8.1$ has been shown over the immediately previous step (without color). In this way the sharp variation between both steps can be observed.

Figure 2 (right) shows the results of analysis of the arch composed of thirteen voussoirs. The solution obtained is similar to the one shown previously in Figure 1. It can be observed that in this case, when the deformation of the left support of the arch increases, the hinge changes twice: when $\bar{v}_z = 2.1$ and when $\bar{v}_z = 5.4$. From this step, if the direction of the displacement is inverted, two different families of solutions are obtained. Both solutions are similar to the one previously obtained in the first arch when $2.5 < \bar{v}_z < 3.6$. Similar solutions to the steps where $\bar{v}_z > 6.4$ in the twelve voussoir arch have not been obtained. However, it is not possible to state that they do not exist. It must be noted that in spite of incorporating the same perturbations in the algorithm, a different solution was obtained. Again, the main solution of Figure 1 has been included with a dashed line so that both results can be compared.

Figure 3 shows the results of the same analysis in the arch with seven (left) and twenty (right) voussoirs. When the number of voussoirs increases — Figure 3 (right) — the discontinuities of the function $f_z =$
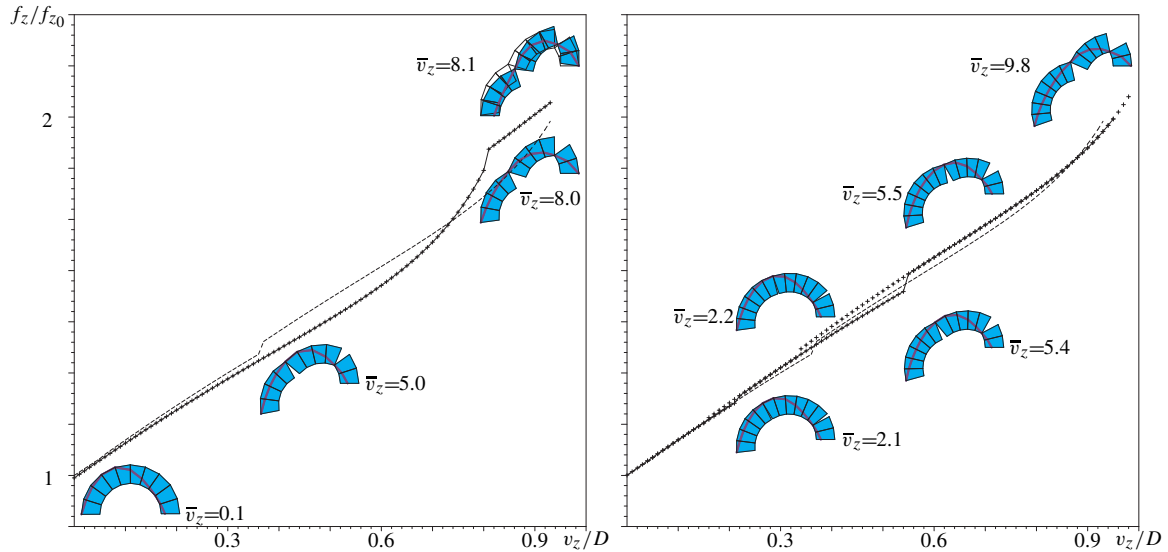
Figure 2. Variation of the vertical reaction in the left support f_z/f_{z_0} depending on the relative displacement $\bar{v}_z/D$ of the arch composed of 10 voussoirs (left) and 13 (right) ($\bar{v}_z = 10v_z/D$).
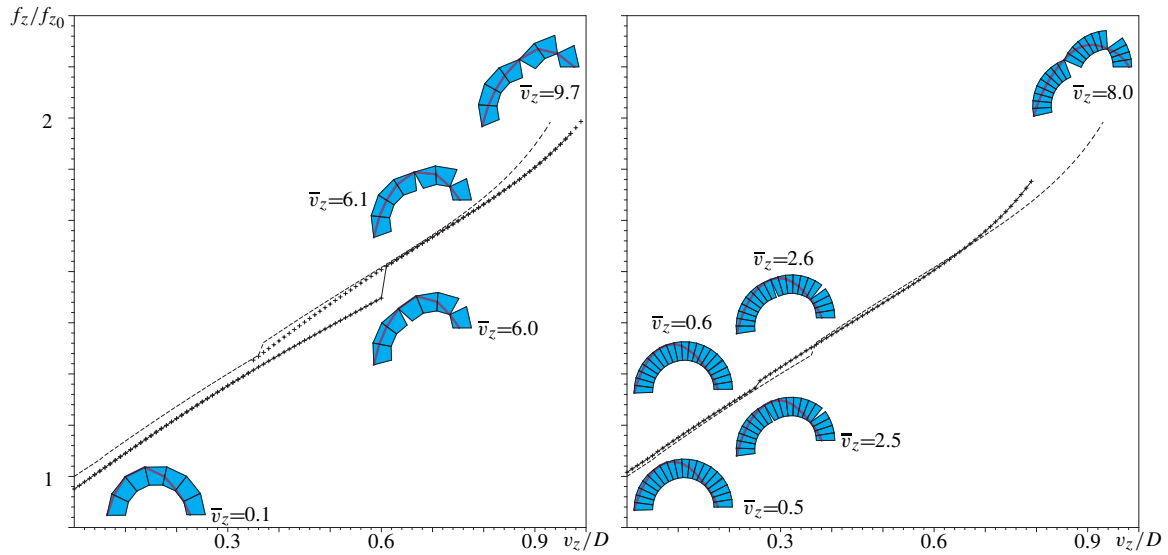

Figure 3. Variation of the vertical reaction in the left support f_z/f_{z_0} depending on the relative displacement $\bar{v}_z/D$ of the arch composed of seven voussoirs (left) and twenty voussoirs (right) ($\bar{v}_z = 10v_z/D$).

$f_z(\bar{v}_z)$ are attenuated. On the other hand, when the number of voussoirs decreases, the effect of the discontinuities increases; see Figure 3 (left). It can be concluded that the decrease of the number of voussoirs increasingly differs from the effect described in [Ochsendorf 2006].

It can be seen that the arch composed of seven voussoirs has a wide range in which two different states

can occur with the same $\bar{v}_z$ value. The second hinge can be located between the third and fourth or fourth and fifth voussoirs. Unlike the results obtained in the twelve voussoir arch, Figure 3 (left) shows that unless a significant perturbation occurs it is not viable to transition from the two states ($3.8 < \bar{v}_z < 6.0$).

Although this work presents the results of an arch with a $5:8$ ratio between its internal and external radii, a previous parametric study carried out in arches showed this ratio varied from $5:6$ to $5:10$. The geometry of the arch studied here corresponds to the proportion which shows the highest hinge variability. For example, in a slender arch with a ratio of $5:6$, these effects are insignificant. Only in models with a high number of voussoirs may some of the hinges vary. It has been shown that in these cases the effect of the variation in the position of the hinges is reduced; see Figure 3 (right). In this slender arch case the solution obtained is unique. Even when a perturbation was included in the algorithm, no variation in the solution arose.

This previous study also explains why this work focuses on the vertical displacement of one of the arch supports. This study shows that the effect of horizontal displacement variation has a minimum influence on the variation of the position of the hinges. When horizontal displacements were applied, only in exceptional cases does an abrupt change in the position of the hinges occur. This effect does not imply that the solution must be unique. In these cases it is simple to obtain alternative solutions. For example, when an arch with an odd number of voussoirs is studied, two different solutions can be obtained depending on whether the hinge is located on one side or the other of the central voussoirs. Although every solution becomes stable (within a certain margin) it is necessary to include perturbations in the algorithm to move from one state to other.

5. Conclusions

The results obtained in this work show the possibility that the position of the opened joints changes along the arch, when the displacement imposed at the support of the arch is modified.

This change of the position of the opened joints spontaneously occurs when the movement of one support gradually increases or decreases. However, when the direction of the movement changes, the abrupt deformation of the arch does not occur at the same point.

Unlike [Ochsendorf 2006], the case studies presented in the present article exhibit multiple solutions. The change from one solution to another can occur when the movement of one support of the arch increases or decreases, but also can occur due to an external perturbation. This phenomenon is shown in the arch of twelve voussoirs studied in Section 4.

The results obtained in this work are specific to the shape (semicircular arch) and slenderness ratio ($5:8$) chosen, and can be hardly generalized. The study of the effect of form and slenderness ratio on the outcome of the progressive settlements deserve further study. The results here presented show a great diversity of qualitative responses that make difficult the possibility of a simple classification.

Currently, also with the aim of seeing if this classification can be done, the present method of calculation offers the possibility to analyze different particular cases of form and slenderness.

Finally, the nonlinear effects observed in the cases studied in this work occur when the movements resultant are definitely large compared to the overall dimensions of the structure. Thus, the solutions obtained with linear formulations, the classic formulation for small movements, is accurate enough for small displacements.

References

[Fishwick 1996] R. J. Fishwick, *Limit analysis of rigid block structures*, Ph.D. thesis, University of Portsmouth, 1996.

[Fortunato et al. 2016] A. Fortunato, E. Babilio, M. Lippiello, A. Gesualdo, and M. Angelillo, "Limit analysis for unilateral masonry-like structures", *Open Constr. Build. Tech. J.* **10**:suppl. 2:M12 (2016), 346–362.

[Fortunato et al. 2018] A. Fortunato, F. Fabbrocino, M. Angelillo, and F. Fraternali, "Limit analysis of masonry structures with free discontinuities", *Meccanica* (*Milano*) **53**:7 (2018), 1793–1802.

[Gilbert and Melbourne 1994] M. Gilbert and C. Melbourne, "Rigid-block analysis of masonry structures", *Struct. Eng.* **72**:21 (1994), 356–361.

[Heyman 1966] J. Heyman, "The stone skeleton", *Int. J. Solids Struct.* **2**:2 (1966), 249–279.

[Heyman 1995] J. Heyman, *The stone skeleton: structural engineering of masonry architecture*, Cambridge Univ. Press, 1995.

[Heyman 2007] J. Heyman, "The plasticity of unreinforced concrete", pp. 157–162 in *Morley symposium on concrete plasticity and its application* (Cambridge, 2007), edited by C. Burgoyne et al., Cambridge Univ. Press, 2007.

[Hu et al. 2012] J. Hu, J. E. Mitchell, J.-S. Pang, and B. Yu, "On linear programs with linear complementarity constraints", *J. Global Optim.* **53**:1 (2012), 29–51.

[Huerta and López 1997] S. Huerta and G. López, "Stability and consolidation of an ashlar barrel vault with great deformations: the church of Guimarei", pp. 587–596 in *Structural studies, repairs and maintenance of historical buildings*, edited by C. A. Brebbia and S. Sánchez-Beitia, WIT Trans. Built Environment **26**, WIT Press, Southampton, 1997.

[Iannuzzo et al. 2018] A. Iannuzzo, M. Angelillo, E. De Chiara, F. De Guglielmo, F. De Serio, F. Ribera, and A. Gesualdo, "Modelling the cracks produced by settlements in masonry structures", *Meccanica* (*Milano*) **53**:7 (2018), 1857–1873.

[Livesley 1978] R. K. Livesley, "Limit analysis of structures formed from rigid blocks", *Int. J. Numer. Methods Eng.* **12**:12 (1978), 1853–1871.

[Magdalena Layos 2013] F. Magdalena Layos, *El problema del rozamiento en el análisis de estructuras de fábrica mediante modelos de sólidos rígidos*, Ph.D. thesis, Universidad Politécnica de Madrid, 2013, https://tinyurl.com/fmlphd.

[Méry 1840] E. Méry, "Mémoire sur l'équilibre des voûtes en berceau", *Annales des Ponts et Chaussées* 19 (1840), 50–70, plates 183–184.

[Ochsendorf 2006] J. A. Ochsendorf, "The masonry arch on spreading supports", *Struct. Eng.* **84**:2 (2006), 29–36.

[Portioli and Cascini 2017] F. Portioli and L. Cascini, "Large displacement analysis of dry-jointed masonry structures subjected to settlements using rigid block modelling", *Eng. Struct.* **148** (2017), 485–496.

JOSÉ IGNACIO HERNANDO GARCÍA: joseignacio.hernando@upm.es
Department of Building Structures and Physics, Universidad Politécnica de Madrid, Madrid School of Arquitecture (ETSAM, UPM), Madrid, Spain

FERNANDO MAGDALENA LAYOS: fernando.magdalena@upm.es
Department of Building Construction, Universidad Politécnica de Madrid, Madrid School of Building Engineering (ETSEM, UPM), Madrid, Spain

ANTONIO AZNAR LÓPEZ: antonio.aznar@upm.es
Department of Building Structures and Physics, Universidad Politécnica de Madrid, Madrid School of Arquitecture (ETSAM, UPM), Madrid, Spain

JOURNAL OF MECHANICS OF MATERIALS AND STRUCTURES

msp.org/jomms

Founded by Charles R. Steele and Marie-Louise Steele

Cover photo: Wikimedia Commons

Special issue on
Structural Analysis
of Real Historic Buildings (part 1)